Supplement of Biogeosciences, 19, 5499–5520, 2022
https://doi.org/10.5194/bg-19-5499-2022-supplement

Biogeosciences Open Access EGU

Supplement of

Tracing the role of Arctic shelf processes in Si and N cycling and export through the Fram Strait: insights from combined silicon and nitrate isotopes

Margot C. F. Debyser et al.

Correspondence to: Margot C. F. Debyser (margot.debyser@ed.ac.uk)

S.1 – Analysis of $\delta^{30}Si(OH)_4$

All analysis of $\delta^{30}Si(OH)_4$ was carried out on a Nu Plasma II MC-ICP-MS at the University of Edinburgh. Analysis was done in pseudo-medium resolution, and the left side of the peak shoulder was measured to separate Si from various N & NO interferences, using a desolvator in pseudo-dry plasma following the configuration in Pichevin et al. (2014). A bracketing of 3 sample measurements with 4 measurements of the isotopic standard NBS28 is used to produce a mean measurement with an estimate of standard deviation, allowing to correct for drift in the instrumentation over time and avoiding subsequent measurement bias. Each analysis is composed of 3 blocks of 15 measurements integrated over 5sec each.

Figure S1 shows the relationship between measured $\delta^{29}Si$ and $\delta^{30}Si$ in samples over the course of the study. A strong relationship is observed between the two isotopes, close to the theoretical kinetic fractionation line. However due to the low DSi concentration and high salt matrix effects from increased precipitation volumes, interference on $\delta^{30}Si$ increased measurement error, reflected in high standard deviations and higher variability in $\delta^{30}Si$ on figure S1. To reduce standard deviations within measurements and improve reliability and global comparability of datasets, $\delta^{29}Si$ was converted to $\delta^{30}Si$ using the theoretical conversion factor of 1.96, calculated from the kinetic fractionation law (Young et al., 2002). Conversion of $\delta^{29}Si$ will not affect general variations in the dataset as most measurements fall within error of the linear relationship observed in figure S1.

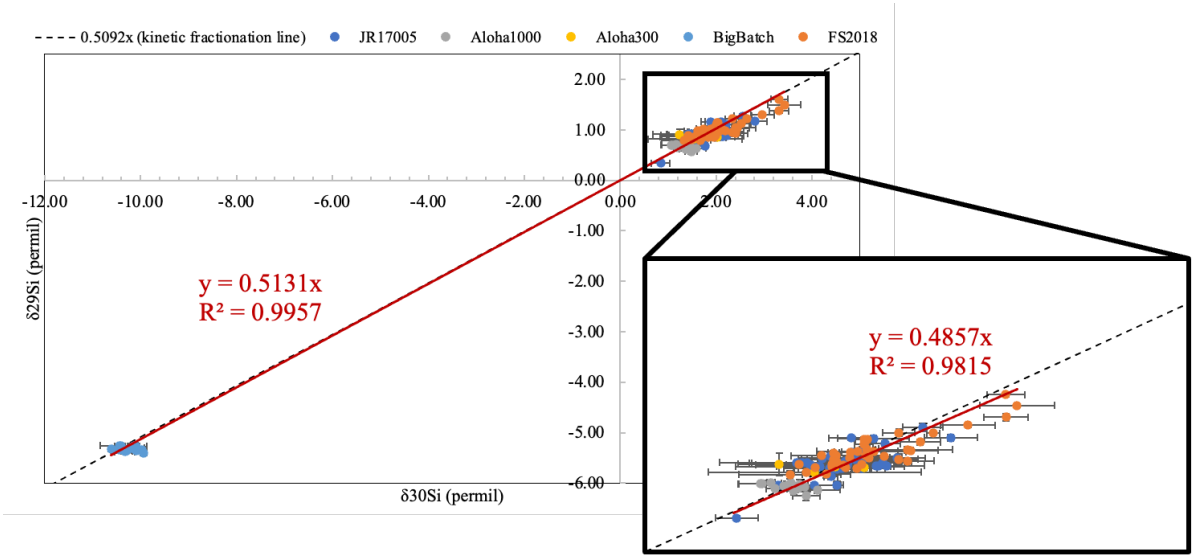

Figure S1. Relationship between $\delta^{29}Si$ and $\delta^{30}Si$ in permil (‰) of all samples and standards over the course of the project. Dotted grey trendline shows the theoretical kinetic fractionation line of 0.5092x (Reynolds et al., 2007). Red line (left) shows the least squared regression for all samples (0.5131, R^2=0.99). Red line on blown up section (right) shows the least squared regression for all seawater samples (0.4857, R^2=0.98).

S.2 – Section of $\delta^{30}Si(OH)_4$ (JR17005)

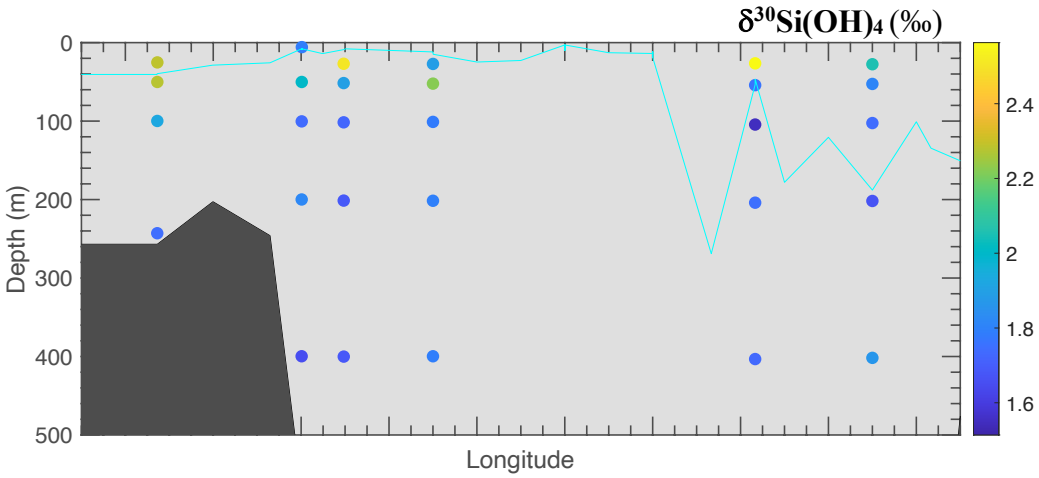

Figure S2. $\delta^{30}Si(OH)_4$ (‰) across the Fram Strait section of spring 2018 (JR17005). Cyan line displays MLD for the section (calculation described in main method section).

S.3 – Isotopic trends in particulate nitrogen and silicon

The nitrogen isotopic composition of particulate nitrogen ($\delta^{15}N$-PN) and the silicon isotopic composition of particulate silicon ($\delta^{30}Si$-PSi) were measured alongside nitrate isotopes and $\delta^{30}Si(OH)_4$ for FS2018 and JR17005 cruises. The methods of collection and analysis is briefly described below. Measurements of $\delta^{15}N$-PN and $\delta^{30}Si$-PSi are shown in the Rayleigh field on Figure S3 and briefly discussed here.

$\delta^{15}N$-PN is very variable but generally high throughout the spring and summer in AW and PSW, highlighting N limitation to local phytoplankton and the shift towards consumption of regenerated nitrogen.

$\delta^{30}Si$-PSi in AW is consistent with the isotopic trends of closed system products and $\delta^{30}Si(OH)_4$ observations that DSi is not resupplied in AW and becomes progressively depleted. $\delta^{30}Si$-PSi in PSW does not follow any fractionation model, consistent with $\delta^{30}Si(OH)_4$ trends which indicate that DSi trends in PSW are driven by mixing rather than biological uptake locally.

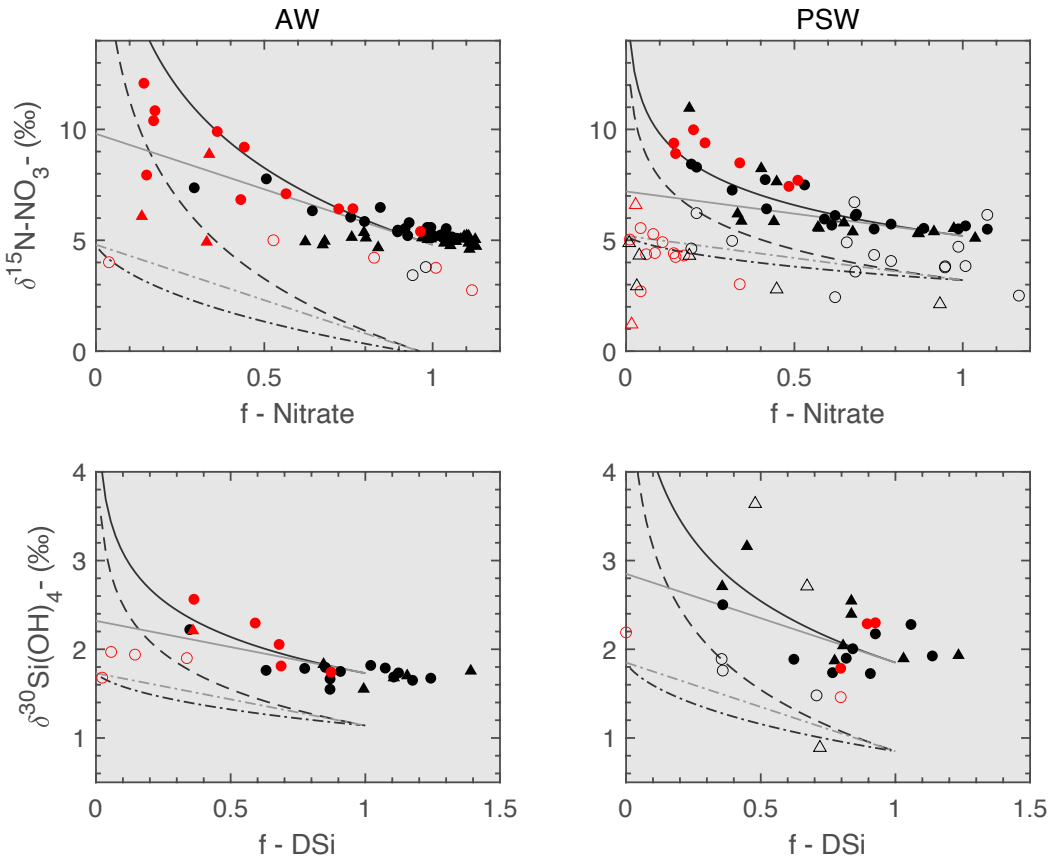

Figure S3. Top panels: nitrate utilisation vs δ^{15}N-NO_3 for AW (left) and PSW (right). Bottom panels: DSi utilisation vs $\delta^{30}Si(OH)_4$ for AW (left) and PSW (right). Circles are denote measurements from JR17005 (spring) and triangles from FS2018 (summer). Red symbols show measurements within the MLD. Black line follows the closed fractionation model and grey line an open fractionation model. Full symbols are seawater measurements, open symbols are for δ^{15}N-PN (above) and δ^{30}Si-PSi (below).

Methods of Analysis

δ^{15}N-PN

Seawater samples were collected from the underway system or niskin bottles into acid-cleaned carboys and filtered through combusted GF/F filters (0.7µM porosity) within 2h of collection on a filtration system. The filters were stored at -80°C until analysis. Prior to analysis the filters were freeze-*dried,* wrapped in tin foil cones (OEA Laboratories) and pelletised. δ^{15}N-PN was determined by EA-IRMS using *a* Costech Instruments Elemental Analyser coupled to Thermo Scientific Delta V Advantage mass spectrometer fitted with Conflo IV gas handling system by Louisa Norman (NOC). The instrumentation was operated using ISODAT 3.0 isotope ratio MS software. L-glutamic acid standards USGS 40 and USGS 41a (US Geological Survey, Reston Stable Isotope Laboratory) were run alongside the samples and were used both for data processing and to assess the performance of the instrumentation.

δ^{30}Si-PSi

Seawater samples were collected from the underway system or niskin bottles into acid-cleaned polyethylene bottles and immediately filtered through nuclepore filters (0.8µM porosity) on a filtration system. The filters were stored at -20°C until analysis. Cleaning and

dissolution of particulate silica was adapted from Morley et al. (2004). Filters were rinsed with MQ and collected particles were dried in digestion vials. 0.5ml of 10% HCl was added to dissolve carbonates overnight and evaporated at 100˚C. 0.2ml of concentrated H_2O_2 was added to dissolve organic compounds overnight and fully evaporated at 120˚C. 1ml of 0.1M NaOH was added to dissolve the particulate silica overnight. Solution was neutralized with HCl and eluted to 5ppm Si. The solution was subsequently processed through resin columns and analysed for $\delta^{30}Si$ on MC-ICP-MS as per the method of analysis of $\delta^{30}Si(OH)_4$ described in the main text's method section.

S.4 – Estimating nutrient sources in Fram Strait

For calculations of f in section 4.2.6, a representative source Arctic shelf DSi concentration of 45µM is used. This is representative of DSi concentrations in Pacific-originating shelf waters (30-40µM Brzezinski et al., 2021; Giesbrecht et al., 2022) and the concentration of DSi exported from rivers into the TPD after burial in estuaries and shelves (47µM, Charette et al., 2020).

Parameters and assumptions used in calculation of section 4.2.6 are as follow:

-Endmember signature composition of riverine DSi = 83µM and $\delta^{30}Si(OH)_4$ = 1.3‰ (Charette et al., 2020; Sun et al., 2018) and upper halocline waters of Pacific influence DSi = 30.6µM and $\delta^{30}Si(OH)_4$ = 1.71‰ (Giesbrecht et al., 2022).

-43% of riverine DSi is removed on shelves prior to transport into the TPD (Charette et al., 2020).

-Mean PSW hydrological composition: 13% meteoric water, 4% Pacific water and 8% sea ice melt. Remaining composition is of Atlantic water (Dodd et al., 2012).

References

Brzezinski, M. A., Closset, I., Jones, J. L., de Souza, G. F. and Maden, C.: New Constraints on the Physical and Biological Controls on the Silicon Isotopic Composition of the Arctic Ocean, Front. Mar. Sci., 8(August), doi:10.3389/fmars.2021.699762, 2021.

Charette, M. A., Kipp, L. E., Jensen, L. T., Dabrowski, J. S., Whitmore, L. M., Fitzsimmons, J. N., Williford, T., Ulfsbo, A., Jones, E., Bundy, R. M., Vivancos, S. M., Pahnke, K., John, S. G., Xiang, Y., Hatta, M., Petrova, M. V., Heimbürger-Boavida, L. E., Bauch, D., Newton, R., Pasqualini, A., Agather, A. M., Amon, R. M. W., Anderson, R. F., Andersson, P. S., Benner, R., Bowman, K. L., Edwards, R. L., Gdaniec, S., Gerringa, L. J. A., González, A. G., Granskog, M., Haley, B., Hammerschmidt, C. R., Hansell, D. A., Henderson, P. B., Kadko, D. C., Kaiser, K., Laan, P., Lam, P. J., Lamborg, C. H., Levier, M., Li, X., Margolin, A. R., Measures, C., Middag, R., Millero, F. J., Moore, W. S., Paffrath, R., Planquette, H., Rabe, B., Reader, H., Rember, R., Rijkenberg, M. J. A., Roy-Barman, M., Rutgers van der Loeff, M., Saito, M., Schauer, U., Schlosser, P., Sherrell, R. M., Shiller, A. M., Slagter, H., Sonke, J. E., Stedmon, C., Woosley, R. J., Valk, O., van Ooijen, J. and Zhang, R.: The Transpolar Drift as a Source of Riverine and Shelf-Derived Trace Elements to the Central Arctic Ocean, J. Geophys. Res. Ocean., 125(5), 1–34, doi:10.1029/2019JC015920, 2020.

Dodd, P. A., Rabe, B., Hansen, E., Falck, E., MacKensen, A., Rohling, E., Stedmon, C. and Kristiansen, S.: The freshwater composition of the Fram Strait outflow derived from a decade of tracer measurements, J. Geophys. Res. Ocean., 117(11), 1–26, doi:10.1029/2012JC008011, 2012.

Giesbrecht, K. E., Varela, D. E., Souza, G. F. and Maden, C.: Natural Variations in Dissolved

Silicon Isotopes Across the Arctic Ocean From the Pacific to the Atlantic, Global Biogeochem. Cycles, 36(5), 1–23, doi:10.1029/2021gb007107, 2022.
Morley, D. W., Leng, M. J., Mackay, A. W., Sloane, H. J., Rioual, P. and Battarbee, R. W.: Cleaning of lake sediment samples for diatom oxygen isotope analysis, J. Paleolimnol., 31(3), 391–401, doi:10.1023/B:JOPL.0000021854.70714.6b, 2004.
Pichevin, L. E., Ganeshram, R. S., Geibert, W., Thunell, R. and Hinton, R.: Silica burial enhanced by iron limitation in oceanic upwellling margins, Nat. Geosci., 7(July), 541–546, doi:10.1038/NGEO2181, 2014.
Reynolds, B. C., Aggarwal, J., André, L., Baxter, D., Beucher, C., Brzezinski, M. A., Engström, E., Georg, R. B., Land, M., Leng, M. J., Opfergelt, S., Rodushkin, I., Sloane, H. J., Van Den Boorn, S. H. J. M., Vroon, P. Z. and Cardinal, D.: An inter-laboratory comparison of Si isotope reference materials, J. Anal. At. Spectrom., 22(5), 561–568, doi:10.1039/b616755a, 2007.
Sun, X., Mörth, C. M., Porcelli, D., Kutscher, L., Hirst, C., Murphy, M. J., Maximov, T., Petrov, R. E., Humborg, C., Schmitt, M. and Andersson, P. S.: Stable silicon isotopic compositions of the Lena River and its tributaries: Implications for silicon delivery to the Arctic Ocean, Geochim. Cosmochim. Acta, 241, 120–133, doi:10.1016/j.gca.2018.08.044, 2018.
Young, E. D., Galy, A. and Nagahara, H.: Kinetic and equilibrium mass-dependent isotope fractionation laws in nature and their geochemical and cosmochemical significance, Geochim. Cosmochim. Acta, 66(6), 1095–1104, doi:10.1016/S0016-7037(01)00832-8, 2002.